IEEE Access
Multidisciplinary ⋮ Rapid Review ⋮ Open Access Journal

Received February 20, 2022, accepted March 20, 2022, date of publication March 23, 2022, date of current version March 28, 2022.

Digital Object Identifier 10.1109/ACCESS.2022.3161748

A Low Dynamic Deviation and High Robustness Position Control Strategy Based on Virtual Reference

TAO LIU[1], QIAOLING TONG[1], (Member, IEEE), QIAO ZHANG[2], (Member, IEEE), AND KAN LIU[3], (Senior Member, IEEE)

[1]School of Optical and Electronic Information, Huazhong University of Science and Technology, Wuhan 430074, China
[2]School of Automation, Wuhan University of Technology, Wuhan 430074, China
[3]College of Mechanical and Vehicle Engineering, Hunan University, Changsha 410082, China

Corresponding author: Qiao Zhang (zqhustcc@163.com)

This work was supported by the National Natural Science Foundation of China under Grant 51877075.

ABSTRACT This paper proposes a modified model predictive control method with the virtual model (VM-MPC) to generate a virtual reference of the position loop. The dynamic deviation is introduced into the virtual reference as a position advance. Applying this virtual reference as the input of position controllers, the dynamic response is greatly improved without changing the gain of position controllers. Therefore, both the dynamic response and robustness of the position loop are improved when the response delay of the speed loop is uncertain. In order to reduce the influence of model mismatch on model predictive control, instead of the actual feedback, a virtual model feedback of the expected position response is used. With this approach, control parameters of VM-MPC are optimized offline to obtain the fast position response without overshoot. A model compensator is proposed to reduce the mismatch between the virtual model and the real system. The effectiveness and feasibility of the proposed method are verified by simulation and experiment results.

INDEX TERMS Model predictive control, virtual reference, robust control, position loop.

I. INTRODUCTION

Permanent magnet synchronous motors (PMSMs) are widely used in servo systems, such as automation equipments, machine tools, and robots due to their high torque density and fast dynamic response. In these applications, the conventional proportional-integral-derivative (PID) control method is popular, thanks to its simple control structure and good control performance [1]–[3]. In order to reduce the overshoot, the proportional-derivative (PD) control method is adopted in the position loop. Usually, the constant setting of PID controllers corresponds only to some specific working ranges without any optimization for changing motor state. In dynamic working conditions and ranges, it will cause the degradation of the response capability or even oscillations.

To solve this problem, some improvement methods based on PID control are proposed, such as fuzzy PID [4]–[6] and model reference adaptive control (MRAC) [7]–[10]. In [6], fuzzy rules are proposed to modify parameters of PID to adapt to different working conditions of servo systems. In [8], an online identification method of MRAC based on fuzzy neural networks is proposed. In these methods, controller parameters are adapted to different working conditions and ranges automatically. However, the parameter tuning process requires a certain length of time, which reduces the robustness of systems. Therefore, more robust methods are proposed, such as robust control [11]–[13], sliding-mode control (SMC) [14]–[17], and backstepping control [18]–[21]. In [12], a robust controller is proposed to achieve the accurate control performance in the presence of plant parameter variations and load disturbances. In [16], an integrated sliding-mode control optimized by different evolution algorithms is proposed to improve the robustness and realize the precision positioning. In [20], a robust position backstepping tracking controller with the extended state observer is proposed. Nevertheless, the dynamic deviation increases with the decreasing of the proportional gain in the position loop. Limited by the robustness constraints, the proportional gain cannot be large enough, which affects the dynamic response of the position loop.

In order to reduce the dynamic deviation and improve the robustness, some feedforward compensation methods are

The associate editor coordinating the review of this manuscript and approving it for publication was Zhong Wu.

proposed, such as speed feedforward compensator [22], [23], active disturbance rejection control (ADRC) [24]–[27], and model predictive control (MPC) [28]–[31]. In [22], the speed feedforward compensator is induced in the position loop to improve the dynamic response. It works well when the reference changes continuously. However, when the step reference is applied, the compensation performance is degraded. In [27], a transient trajectory generator and the extended state observer are proposed to improve the dynamic response and the anti-disturbance capability of position servo systems. Although the tracking error is reduced by these methods, physical constraints of different systems are not considered, such as torque and speed limitations. These constraints affect the dynamic response of real systems and cause the mismatch between the designed response capability and that of real systems. Due to characteristics of MPC that these constraints are especially considered, MPC has been applied in the speed and current control of motor drives successfully [32], [33]. In [31], a cost function with optimized prediction horizons is proposed for PMSM driving of position control applications. Thanks to the predictive performance of MPC, this method has been applied in trajectory optimizations. However, the control performance of MPC is affected by model parameters. In the position tracking application, the response delay of the speed loop is uncertain, which restricts the application of MPC.

To improve the dynamic response and robustness at the same time, a virtual reference trajectory generator based on virtual-model-based model predictive control (VM-MPC) is proposed. In this strategy, the small gain of the position controller is selected to improve the robustness and a virtual reference trajectory with the position advance is generated to improve the dynamic response. The virtual model, instead of the actual position system, is used in MPC to generate the virtual reference trajectory. With this approach, the influence of the speed loop response delay on MPC is reduced and controller parameters can be optimized offline to avoid the position overshoot. The virtual reference is obtained by minimizing the dynamic error between the actual reference and the virtual model feedback. Moreover, the dynamic deviation is introduced into the virtual reference as a position advance. Applying this virtual reference as the input of position controllers, the position tracking with low dynamic deviation is obtained. In order to compensate the mismatch between the virtual model and the actual system, a model compensator (MC) is used. The mechanical response of servo systems is considered as constraints of VM-MPC. The proposed method can be easily adapted to different systems by modifying the expected response bandwidth and constraints. There are two main contributions of this paper. One is an optimized virtual reference trajectory generation method with the position advance is proposed to reduce the dynamic deviation in the position control. With this approach, both the robustness and dynamic response are improved. The other is a virtual model is induced in MPC to reduce the influence of model mismatch. Therefore, the improved VM-MPC method is more robust.

The paper is organized as follows. In section II, the mathematical model of the position loop is introduced. In section III, the proposed VM-MPC and MC are explained in detail. In section IV, the proposed method is compared with other methods through experiment and simulation results. Finally, conclusions of this paper are shown in section V.

II. THE MATHEMATIC MODEL OF THE POSITION LOOP

According to the mechanical equation of PMSM, the ideal mathematic models of the speed loop and the position loop are shown as:

$$Js\omega = T_e - T_L, \tag{1}$$

$$s\theta = \omega, \tag{2}$$

where J is the moment of inertia, ω is the mechanical speed, T_e is the electromagnetic torque, T_L is the load torque, and θ is the mechanical angle.

When the response delay of the speed loop is ignored, the control structure of the position loop is shown in Fig. 1. The closed-loop transfer function of it can be expressed as:

$$G_p(s) = \frac{\theta_f}{\theta_r} = \frac{K_p}{K_p + s}, \tag{3}$$

where K_p is the proportional gain, θ_r is the reference angle, and θ_f is the angle feedback. It is a first-order low-pass filter and its cut-off frequency is expressed as α_{pn}. Therefore, the expected response model of the position loop is expressed as:

$$\theta_f = \frac{\alpha_{pn}}{\alpha_{pn} + s}\theta_r, \tag{4}$$

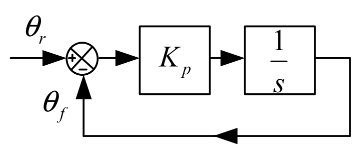

FIGURE 1. The control block diagram of the position loop.

The amplitude-frequency characteristic diagram of the position loop when considering the speed loop response bandwidth is shown in Fig. 2. The expected response bandwidth of the position loop (α_{pn}) is 80rad/s. It can be seen from Fig. 2 that when the response bandwidth of the speed loop is much larger than that of the position loop, the amplitude response characteristic of the position loop is close to the ideal response results in (4). When the response bandwidth of the speed loop is reduced, the amplitude response characteristic in the middle frequency region begins to deviate from ideal response results. Moreover, the amplitude response is larger than 0dB, resulting in the position overshoot.

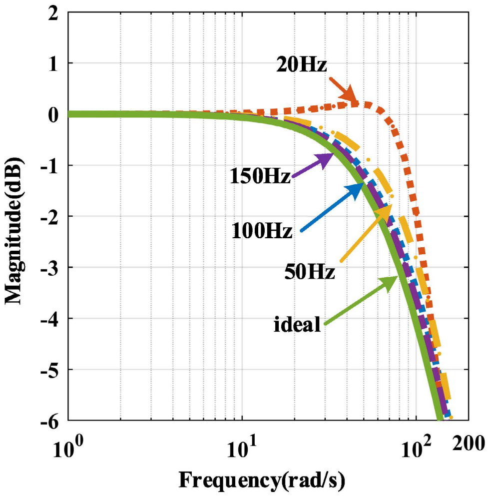

FIGURE 2. The amplitude-frequency characteristic diagram of the position loop with different speed loop response bandwidths (α_{pn} = 80rad/s).

The amplitude-frequency characteristics of the position loop with different position controller gains are shown in Fig. 3, where the speed loop response bandwidth is 50Hz. When the position controller gains are small, the dynamic response of the position loop degrades without overshoot. When the position controller gains are large, the dynamic response of the position loop improves, but the overshoot appears. Combining the results of Fig. 2 and Fig. 3, it can be seen that when the controller gains of the position loop are small, it is less affected by the response bandwidth of the speed loop and has good robustness. When the controller gains of the position loop are large, the dynamic response of the position loop is good, but it is easily affected by the response bandwidth of the speed loop. Therefore, the position controller gains need to be comprehensively selected between the dynamic response and robustness.

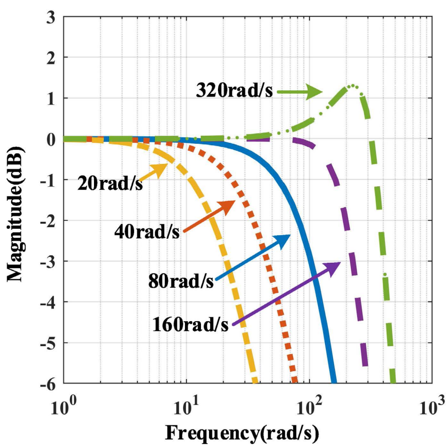

FIGURE 3. The amplitude-frequency characteristic diagram of the position loop with different position controller gains.

III. THE PROPOSED VM-MPC STRATEGY

Since the expected response model of the position loop can be simplified as a first-order low-pass filter and selected as the virtual model, a virtual reference is generated according to the feedback of the virtual model instead of that of the real system. With this approach, the influence of the speed loop response bandwidth on MPC is reduced. The position reference trajectory is designed in the proposed VM-MPC strategy to guarantee the dynamic error between the feedback of the virtual model and the actual reference as small as possible. The dynamic deviation is introduced into the virtual reference as a position advance. Applying this virtual reference as the input of position controllers, the position tracking with low dynamic deviation is obtained. The details of VM-MPC are explained in section A.

A. VIRTUAL-MODEL-BASED MODEL PREDICTIVE CONTROL

The virtual model is the expected response model of the position loop and it is expressed as:

$$\theta_{mf} = \frac{\alpha_{pn}}{\alpha_{pn} + s}\theta_{vr}, \tag{5}$$

where θ_{mf} is the position feedback of the virtual model and θ_{vr} is the virtual reference. Selecting the virtual reference as control variables, the discretized state-space equation of VM-MPC is obtained as:

$$\begin{aligned} \theta_{mf}(k+1) &= (1-\alpha_{pn}T_s)\theta_{mf}(k) + \alpha_{pn}T_s\theta_{vr}(k) \\ &= Ax(k) + Bu(k), \end{aligned} \tag{6}$$

$$\begin{aligned} y(k) &= \theta_{mf}(k) \\ &= Cx(k), \end{aligned} \tag{7}$$

where T_s is the sampling period.

Taking $X = \begin{bmatrix} \Delta x & y \end{bmatrix}^T$, $Y = y$, the augmented state-space equation is expressed as:

$$\begin{aligned} X(k+1) &= \begin{bmatrix} 1-\alpha_{pn}T_s & 0 \\ 1-\alpha_{pn}T_s & 1 \end{bmatrix} \begin{bmatrix} \Delta\theta_{mf}(k) \\ \theta_{mf}(k) \end{bmatrix} \\ &\quad + \begin{bmatrix} \alpha_{pn}T_s \\ \alpha_{pn}T_s \end{bmatrix} \Delta\theta_{vr}(k) \\ &= A_m X(k) + B_m \Delta u(k), \end{aligned} \tag{8}$$

$$\begin{aligned} Y(k) &= \begin{bmatrix} 0 & 1 \end{bmatrix} \begin{bmatrix} \Delta\theta_{mf}(k) \\ \theta_{mf}(k) \end{bmatrix} \\ &= C_m X(k), \end{aligned} \tag{9}$$

If the prediction horizon is nT_s ($n \geq 1$) and the control horizon is dT_s ($1 \leq d \leq n$), the predictive output variables can be deduced based on the state-space equation as given in (8) and (9):

$$\begin{aligned} Y(k+n|k) &= C_m A_m^n x(k) + C_m A_m^{n-1} B_m \Delta u(k) + \ldots \\ &\quad + C_m A_m^{n-d} B_m \Delta u(k+d-1), \end{aligned} \tag{10}$$

The predictive position sequence over a prediction horizon is $\hat{Y} = \begin{bmatrix} Y(k+1|k) & Y(k+2|k) & \ldots & Y(k+n|k) \end{bmatrix}^T \in \mathbb{R}^n$, and the control sequence over a control horizon is

$\Delta U = \left[\Delta u(k)\ \Delta u(k+1) \ldots \Delta u(k+d-1) \right]^T \in \mathbb{R}^d$. Therefore, the predictive model can be expressed as:

$$\hat{Y} = FX(k) + \Phi \Delta U, \tag{11}$$

where $F = \left[C_m A_m\ C_m A_m^2 \ldots C_m A_m^n \right]^T$,

$$\Phi = \begin{bmatrix} C_m B_m & 0 & 0 & 0 \\ C_m A_m B_m & C_m B_m & 0 & 0 \\ \ldots & \ldots & C_m B_m & 0 \\ C_m A_m^{n-1} B_m & C_m A_m^{n-2} B_m & \ldots & C_m A_m^{n-d} B_m \end{bmatrix}.$$

If the actual reference over a prediction horizon is $R_s = \bar{R}_s \theta_r(k)$, the cost function of this system is obtained as:

$$J = (R_s - \hat{Y})^T (R_s - \hat{Y}) + \Delta U^T R \Delta U, \tag{12}$$

where $\bar{R}_s = \left[1 \ldots 1 \right]^T_{1 \times n}$, R is the weighting matric of control variables and it is expressed as:

$$R = \begin{bmatrix} r & \cdots & 0 \\ \vdots & \ddots & \vdots \\ 0 & \cdots & r \end{bmatrix} \in \mathbb{R}^{d \times d}.$$

The cost function is used to optimize the control sequence ΔU and only the first element of the control sequence is applied. The optimal control sequence is obtained by minimizing the cost function and it is expressed as:

$$\frac{\partial J}{\partial \Delta U} = -2\Phi^T (R_s - FX(k)) + 2(\Phi^T \Phi + R)\Delta U = 0, \tag{13}$$

$$\Delta U = (\Phi^T \Phi + R)^{-1} \Phi^T [R_s - FX(k)]. \tag{14}$$

The first element of the optimized control sequence is obtained as:

$$\begin{aligned} \Delta u(k) &= \left[1\ 0 \ldots 0 \right]_{1 \times d} \Delta U \\ &= K_y \theta_r(k) - K_{mpc} X(k), \end{aligned} \tag{15}$$

where K_y is the first element of $(\Phi^T \Phi + R)^{-1} \Phi^T \bar{R}_s$, K_{mpc} is the first row of $(\Phi^T \Phi + R)^{-1} \Phi^T F$. Since elements in the last column of F are 1, the last element of K_{mpc} is equal to K_y. Equation (15) is simplified as:

$$\Delta u(k) = K_y(\theta_r(k) - \theta_{mf}(k)) - K_{mpc1} \Delta \theta_{mf}(k), \tag{16}$$

where K_{mpc1} is the first element of K_{mpc}.

In real systems, the mechanical speed is a constrained quantity. In order to avoid overshoot, the position advance of the virtual reference need to be constrained. Therefore, constraints of this method are shown as:

$$\begin{cases} |\Delta u| \leq \omega_{\max} T_s \\ |\theta_{vr} - \theta_r| < \theta_{\max}, \end{cases} \tag{17}$$

where ω_{max} is the maximum limitation value of the speed and θ_{max} is the maximum value of the position advance.

According to the backward difference equation, (16) can be rewritten as:

$$s\theta_{vr} = K_y / T_s (\theta_r - \theta_{mf}) - K_{mpc1} s \theta_{mf}, \tag{18}$$

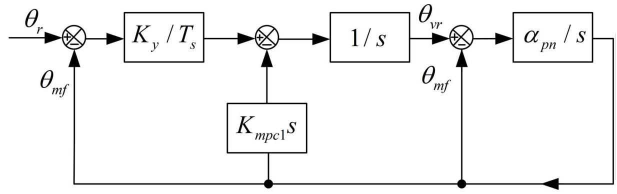

FIGURE 4. The control block diagram of VM-MPC.

Fig. 4 shows the control block diagram of VM-MPC according to (18) and (5). A virtual model of the position loop is used to obtain the ideal position feedback which not affected by the uncertain response delay of the speed loop. According to the ideal feedback, the virtual reference is generated by MPC method to minimize the dynamic error between the actual reference and the ideal feedback. Applying the virtual reference to real systems, the actual dynamic error between the actual reference and the actual feedback is reduced by the position advance in the virtual reference. With this approach, the actual dynamic error is reduced without changing controller gains of the position loop.

B. STABILITY OF VM-MPC

After the VM-MPC method is proposed, the stability of it need to be discussed. According to (18) and (5), the state-space equation of VM-MPC is expressed as:

$$\begin{aligned} \begin{bmatrix} \dot{\theta}_{vr} \\ \dot{\theta}_{mf} \end{bmatrix} &= \begin{bmatrix} -K_{mpc1}\alpha_{pn} & K_{mpc1}\alpha_{pn} - \frac{K_y}{T_s} \\ \alpha_{pn} & -\alpha_{pn} \end{bmatrix} \begin{bmatrix} \theta_{vr} \\ \theta_{mf} \end{bmatrix} + \begin{bmatrix} \frac{K_y}{T_s} \\ 0 \end{bmatrix} \theta_r \\ &= A_1 x_1 + B_1 \theta_r, \end{aligned} \tag{19}$$

The closed-loop system is stable if the eigenvalues of matrix A_1 are nonpositive. The eigenvalues of A_1 are calculated as:

$$\begin{aligned} |\chi I - A_1| &= \left| \begin{bmatrix} \chi + K_{mpc1}\alpha_{pn} & \frac{K_y}{T_s} - K_{mpc1}\alpha_{pn} \\ -\alpha_{pn} & \chi + \alpha_{pn} \end{bmatrix} \right| \\ &= \chi^2 + \alpha_{pn}(K_{mpc1} + 1)\chi + \frac{\alpha_{pn} K_y}{T_s}. \end{aligned} \tag{20}$$

In order to make the eigenvalues nonpositive, the following conditions need to be met:

$$\begin{cases} \alpha_{pn}(K_{mpc1} + 1) \geq 0 \\ \alpha_{pn} K_y / T_s \geq 0. \end{cases} \tag{21}$$

Due to $\alpha_{pn} > 0$, the mentioned conditions are rewritten as:

$$\begin{cases} K_{mpc1} \geq -1 \\ K_y \geq 0. \end{cases} \tag{22}$$

These conditions can be achieved by adjusting the prediction horizon nT_s, the control horizon dT_s and the weight matrix R.

C. THE MODEL COMPENSATOR

Due to the response delay of the speed loop is not considered in the virtual model, the response deviation between the virtual model and real systems is introduced. To reduce the deviation, the model compensator is proposed. According to Fig. 5, the closed-loop transfer function is expressed as:

$$G_m(s) = \frac{\theta_f(s)}{\theta_{mf}(s)} = \frac{\alpha_{pn} + s + G_{mc}(s)}{T_f s^2 + \alpha_{pn} + s + G_{mc}(s)}. \tag{23}$$

where T_f is the equivalent delay time of the speed loop. G_{mc} is the model compensator of the position loop and it is expressed as:

$$G_{mc}(s) = K_{pmc}. \tag{24}$$

Therefore,

$$\begin{aligned} G_m(s) &= \frac{s + (K_{pmc} + \alpha_{pn})}{T_f s^2 + s + (K_{pmc} + \alpha_{pn})} \\ &= \frac{1/T_f s + (K_{pmc} + \alpha_{pn})/T_f}{s^2 + 1/T_f s + (K_{pmc} + \alpha_{pn})/T_f}. \end{aligned} \tag{25}$$

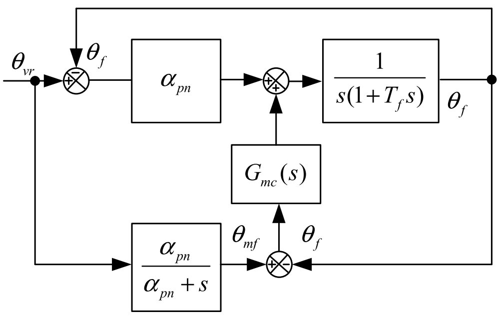

FIGURE 5. The control block diagram of the model compensator.

If the poles of G_m are same and the value of them is α_{mn}, parameters of the model compensator are obtained as:

$$\begin{cases} \alpha_{mn} = 1/(2T_f) \\ K_{pmc} = 1/(4T_f) - \alpha_{pn}. \end{cases} \tag{26}$$

Due to the delay time of the speed loop is difficult to be determined, T_f is replaced by the expected response bandwidth of the speed loop (α_{sn}). The parameter of the model compensator is finally obtained as:

$$K_{pmc} = \alpha_{sn}/4 - \alpha_{pn}. \tag{27}$$

D. PARAMETER TUNING

Fig. 6 shows the control block diagram of the position loop based on the proposed strategy. The proposed virtual reference generator based on VM-MPC is placed between the actual reference and the position controller to reduce the dynamic deviation in the position tracking process. Instead of the actual reference, the virtual reference is used as inputs of the position controller. Therefore, the dynamic deviation is reduced by the position advance in the virtual reference. Moreover, a model compensator is used to reduce the deviation between the virtual model and real systems. Considering the response time of mechanical systems, the control period of VM-MPC is selected as 1ms. The prediction horizon is $30T_s$ and the control horizon is $2T_s$. After that, the parameter needs to be determined is the weight value (r).

Due to parameters of Φ and F are const values when the position controller gains are determined. Therefore, values of K_y and K_{mpc1} can be calculated offline or in the initial stage, which will not cost computing resources during the control cycle. Fig. 7 shows the variation of K_y and K_{mpc1} with r where α_{pn} is 30rad/s. In the displayed value ranges, the stability conditions shown in (22) is always met. The values of K_y and K_{mpc1} increase monotonically as r decreases. In order to minimize the position dynamic error and avoid overshoot, the value of r needs to be selected reasonably.

To avoid the position overshoot of the actual feedback, the virtual reference needs to be adjusted to guarantee the virtual model feedback without overshoot. According to equation (5) and (18), the transfer function between the virtual model feedback and the actual reference is obtained as:

$$G(s) = \frac{\theta_{mf}}{\theta_r} = \frac{K_y \alpha_{pn}/T_s}{s^2 + (1 + K_{mpc1}\alpha_{pn})s + K_y \alpha_{pn}/T_s}. \tag{28}$$

Fig. 8 shows the amplitude-frequency characteristic diagram of (28) with different values of r. It can be seen from Fig. 8 that the response bandwidth increases with the decreasing of r. This means that the dynamic error between the virtual feedback and the real reference is reduced by choosing the lower value of r. However, when the value of r is further reduced, the feedback amplitude in the mid-frequency region is larger than 0dB. This means that the virtual feedback amplitude is larger than the actual reference amplitude, resulting in the position overshoot. In order to minimize the dynamic error and avoid overshoot, the value of r is selected as 0.04 in this paper. There are two constraints in (17), one is the maximum speed constraint and the other is the maximum position advance. The maximum speed constraint is selected as the maximum operating speed of the test motor. The maximum operating speed is 300rad/s. The maximum position advance is selected according to experiment and simulation results with the step reference excitation. When the maximum position advance is too small, the position dynamic deviation is large. When the maximum position advance is too large, the overshoot appears at the end of the positioning process. Through this tuning method, 2.5rad was selected.

IV. SIMULATION AND EXPERIMENT RESULTS

To verify the effectiveness of the proposed strategy, simulations and experiments are carried out. The simulation system is built in Simulink/MATLAB and the experimental platform is shown in Fig. 9. The proposed control strategy is implemented in an ARM MCU (STM32F446VC). The encoder number of the test motor is 10000 pulse/rev and the switch frequency of the servo driver is 10kHz. Parameters of the test system in simulations and experiments are shown in Table 1. Due to only the first element of the control sequence is applied in the real system, which is shown in (16).

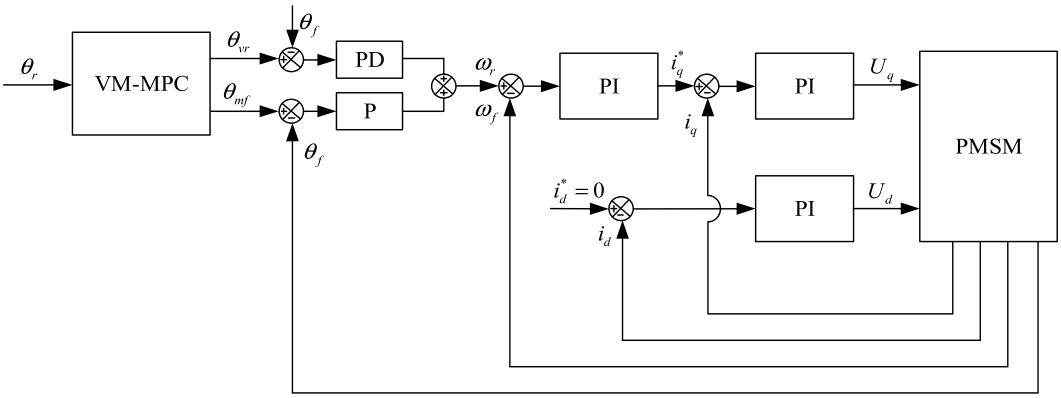

FIGURE 6. The control block diagram of the position control based on VM-MPC and MC.

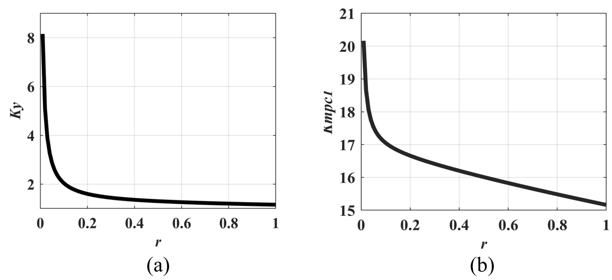

FIGURE 7. The variation of K_y (a) and K_{mpc1} (b) with r (α_{pn} = 30rad/s).

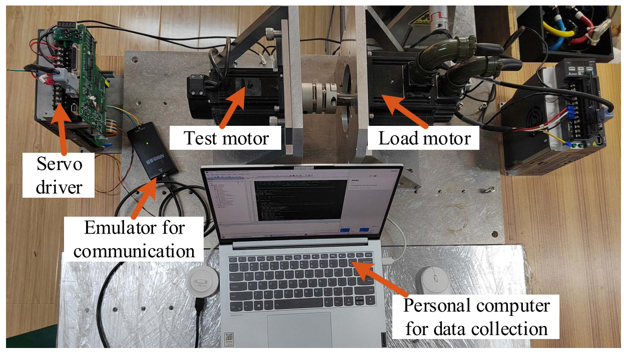

FIGURE 9. The experimental platform.

TABLE 1. Parameter of the test system.

Symbol	Parameters	Value
T_s	control period	1ms
N_p	prediction sequence length	30
N_c	control sequence length	2
α_{pn}	response width of position loop	30rad/s
α_{sn}	response width of speed loop	100Hz
r	weight value	0.04
K_y	gain of VM-MPC	3.26
K_{mpc1}	gain of VM-MPC	17.75
K_{pmc}	gain of MC	120rad/s

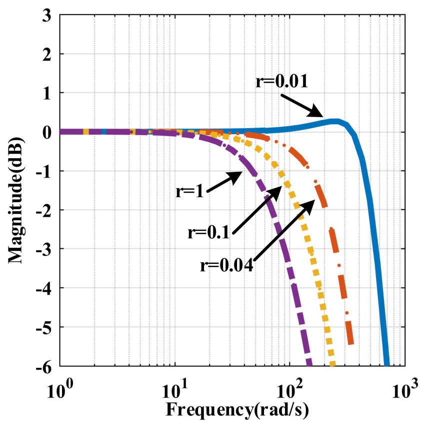

FIGURE 8. The amplitude-frequency characteristic diagram with different values of r.

Moreover, values of K_y and K_{mpc1} can be calculated offline or in the initial stage as mentioned before. Therefore, only two multiplication operations and some addition or subtraction operations of VM-MPC are needed in the control cycle.

Some similar position control methods are selected as comparisons, such as MPC, proportional-derivative control (PD), and proportional control with speed feedforward compensation (PF). Control parameters of these methods are shown in Table 2. To simplify the presentation, PD with high controller gains is abbreviated as PD-H and PF with high controller gains is abbreviated as PF-H.

A. SIMULATION RESULTS

Fig. 10 shows the position tracking waveforms of different methods. The PD method without the virtual reference is selected as a comparison. It can be seen from Fig. 10(a) that the virtual reference leads the actual reference in the proposed VM-MPC results. When the virtual reference is applied, the position feedback tracks the real position trajectory closely. However, there is a large dynamic tracking error in the comparative PD results. This difference can be explained by results of Fig. 10(b). There are two dynamic tracking errors

TABLE 2. Parameters of comparison method.

Method	Symbol	Parameters	Value
MPC	K_{vm}	gain of MPC	6.86
	K_{mpc1m}	gain of MPC	139.04
VM-MPC	K_p	proportional gain	30
	K_d	derivative gain	0.6
PD-H	K_{p1}	proportional gain	110
	K_{d1}	derivative gain	0.6
PD	K_{p2}	proportional gain	30
	K_{d2}	derivative gain	0.6
PF-H	K_{p3}	proportional gain	60
	K_{f3}	feedforward gain	0.6
PF	K_{p4}	proportional gain	30
	K_{f4}	feedforward gain	0.6

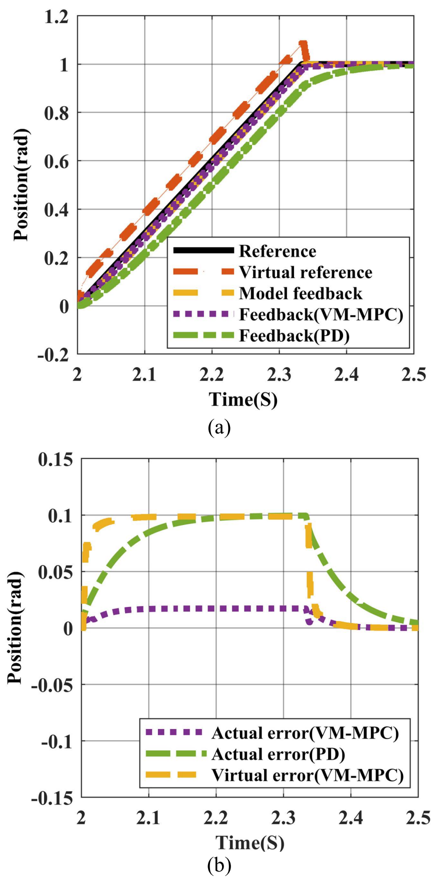

FIGURE 10. The position tracking waveforms of VM-MPC and PD method.

of VMMPC, one is the error between the actual reference and the actual feedback, which is shown as the purple line and is named as the actual error. The other is the error between the virtual reference and the actual feedback, which is shown as the yellow line and is named as the virtual error. The dynamic tracking error of PD is the actual error between the actual reference and the actual feedback, which is shown as the green line. In the position control, due to the output speed reference is proportional to the dynamic tracking error and controller gains of VMMPC and PD are the same. The maximum dynamic tracking errors of VMMPC and PD are the same when the output speed reference is equal to the command speed. The maximum dynamic tracking error of PD is the actual error and the maximum dynamic tracking error of VMMPC is the virtual error. In the initial process of the position tracking, the virtual error of VMMPC is larger than the actual error of PD due to the rapid rise of the virtual reference. This improves the dynamic tracking capability of VMMPC. It can be seen from Fig. 10(b) that the actual error of VMMPC is much smaller than that of PD, which thanks to the position advance in the virtual reference.

B. EXPERIMENT RESULTS

Fig. 11 shows the step response results of different methods. To quantitatively compare the transient and steady-state performance between the proposed method and other methods, different performance indices such as the rise time (with the 100pulse error bound), the settling time (with the 10pulse error bound), the overshoot and the steady state fluctuation are given in Table 3. Compared with PD and PF methods, results of PD-H and PF-H have the much shorter rise time and the settling time. This improvement is achieved by increasing controller gains. However, results of VM-MPC have the similar rise time and the settling time to that of

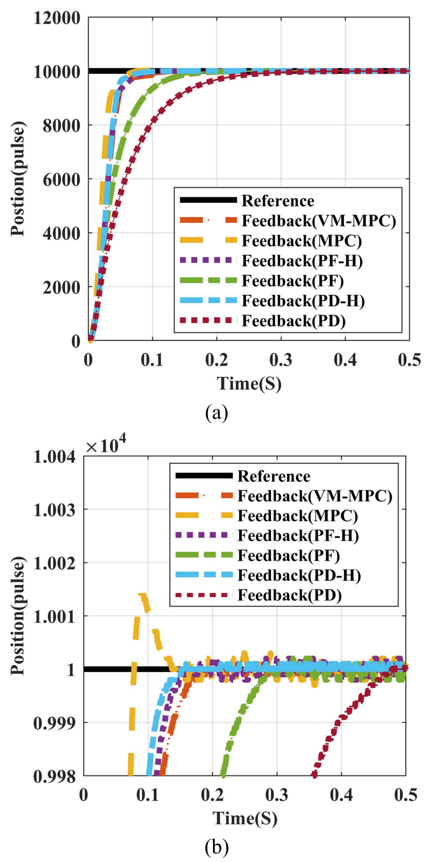

FIGURE 11. The step response of different methods: (a) dynamic results and (b) steady state results.

TABLE 3. Step response results of different methods.

Control method	Rise time (s)	Settling time (s)	Overshoot (pulse)	Steady state fluctuation (pulse)
VM-MPC	0.083	0.138	1	±1
MPC	0.064	0.102	14	±2
PD-H	0.075	0.111	1	±1
PD	0.266	0.394	1	±1
PF-H	0.087	0.125	1	±1
PF	0.162	0.238	1	±1

TABLE 4. Slope response results of different methods.

Control method	Rise time (s)	Settling time (s)	Overshoot (pulse)	Maximum dynamic error (%)
VM-MPC	0.111	0.186	1	8.73
MPC	0.136	0.163	10	20.18
PD-H	0.143	0.180	1	16.71
PD	0.313	0.441	1	43.51
PF-H	0.146	0.184	1	16.20
PF	0.209	0.284	1	27.88

PF-H and PD-H results. And controller gains of VM-MPC are the same as that of PF and PD methods. It means that the step dynamic response is improved by the proposed method without changing the position controller gains. Both using the virtual reference generated by the virtual response model and model compensator contribute to the improvement of response capability. The results of MPC method have the shortest rise time and settling time, but has a slight overshoot. The steady state fluctuations of these methods are within 2pulse. This means these methods have good steady-state characteristics.

Fig. 12 shows the slope response results of different methods. Performance parameters are shown in Table 4. Compared with PD and PD-H methods, PF and PF-H methods have the better dynamic response capability. The compensation result of the speed feedforward is much better in the slope reference than that in the step reference. This means that the dynamic response is improved by the speed feedforward compensator when the reference is changed continuously. It can be seen from results of PD and PD-H, PF and PF-H methods, the dynamic response capability is improved by increasing the proportional gain. It can be seen form Fig. 12 and Table 4 that the rise time and the maximum dynamic error of VM-MPC results are smallest. This means that the dynamic tracking ability of VM-MPC results is better. It is significantly different from results of the step response. The improvement of VM-MPC results is due to the position advance in the virtual reference. When the slope reference is used, the virtual reference of VM-MPC leads the actual reference, which does not appear in the compared control methods. This greatly improves the dynamic tracking capability of the position loop. The maximum dynamic error of MPC is quite large, but the settling time is shortest. This shows that MPC method has excellent performance in the end of the positioning process, but the dynamic tracking deviation is still limited by gains of MPC. The steady state fluctuations of these methods in slope response results are similar to that in step response results, which steady state fluctuations are within 2pulse.

Fig. 13 shows response results of different methods with the reference of sinusoidal signal (5Hz). The amplitude

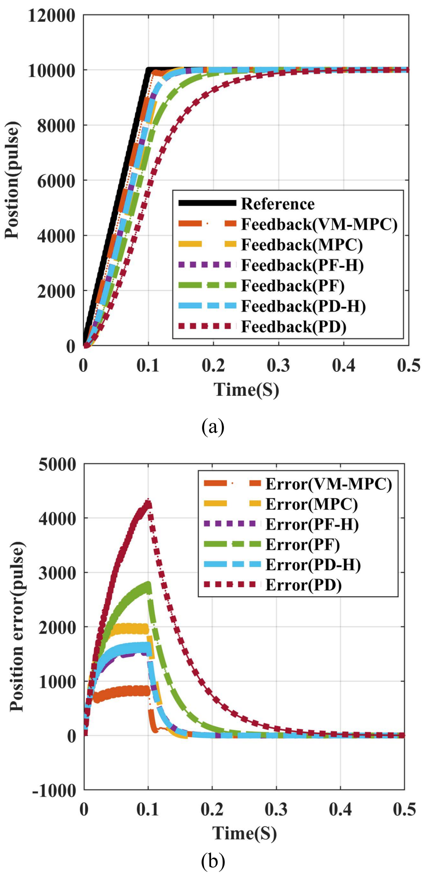

FIGURE 12. **The slope response of different methods: (a) dynamic results and (b) steady state results.**

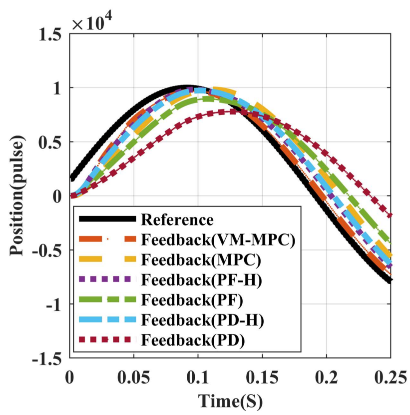

FIGURE 13. **The response of different methods with the sinusoidal excitation (5Hz).**

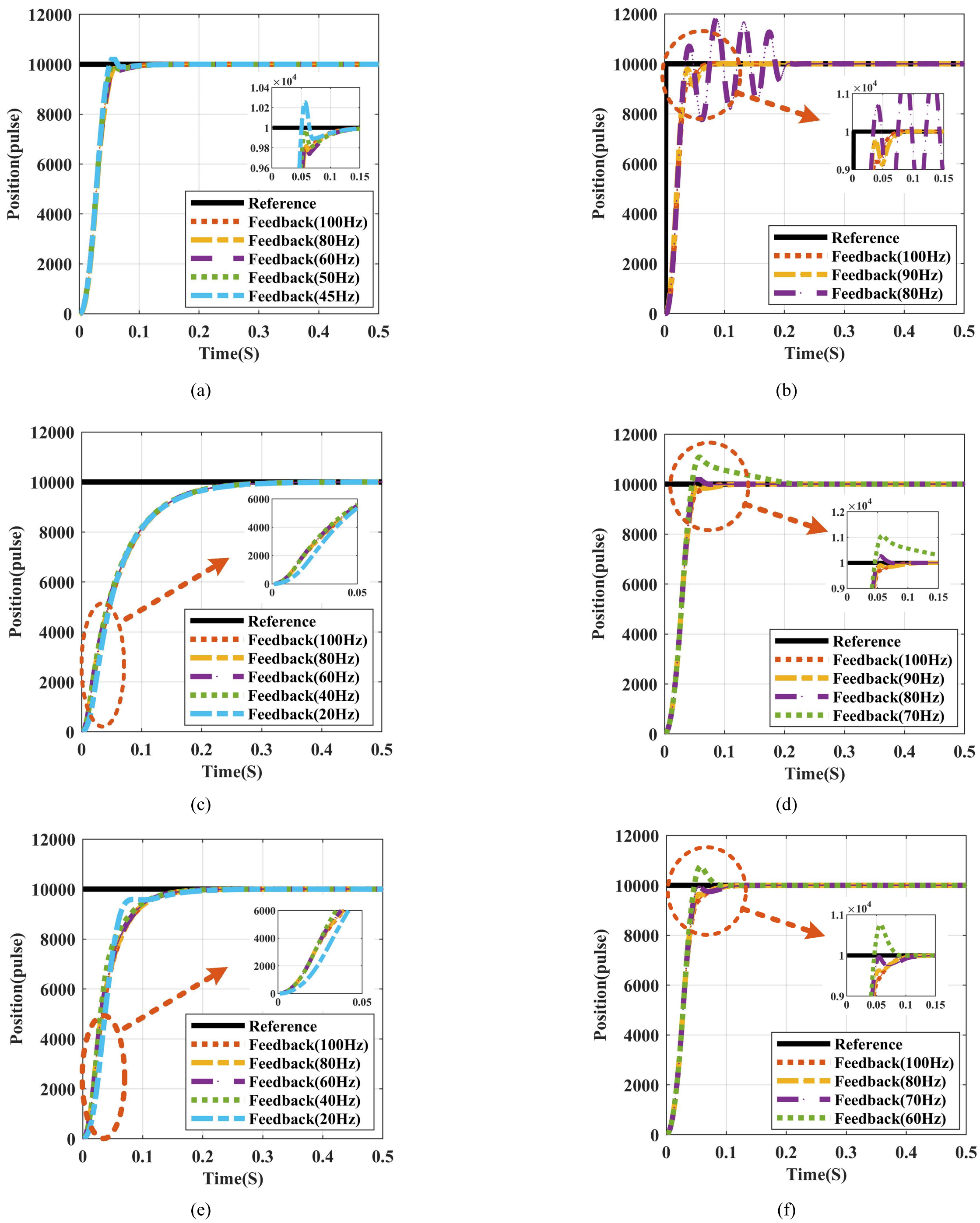

FIGURE 14. Robustness test results of (a) VM-MPC, (b) MPC, (C) PD, (d) PD-H, (e) PF, and (f)PF-H with different speed loop response bandwidths.

attenuations and phase lags of VM-MPC, MPC, PD-H, and PF-H are similar. When the sinusoidal signal reference is applied, these methods maintain better dynamic performance. Compared with PF and PD method, he response capability of servo systems is improved both by the feedforward compensator and VM-MPC, thereby reducing the amplitude attenuations. Especially when the proposed virtual reference is applied, the amplitude of the position feedback is almost non-attenuated. From different forms of reference response results, it shows that the dynamic response of servo systems is improved by the proposed method without changing controller gains.

Although there are different methods to improve the dynamic response of the position loop, the robustness of different methods is different. Fig. 14 is experiment results of different methods when the response bandwidths of the speed loop are changed. The speed loop is a part of the position loop and its response bandwidth affects parameters of the position loop. Controller parameters of different methods are selected when the speed loop response bandwidth is 100Hz. This value is an intermediate value that the test system can achieve. By changing the speed loop response bandwidth, the control performance variations of different methods are carried out when parameters of the position loop are changed. It can be seen from Fig. 14(a) that when the response bandwidth of the speed loop is changed from 100Hz to 50Hz, step response results of VM-MPC are similar and without overshoot. When the response bandwidth is reduced to 45Hz, the overshoot appears at the end of the positioning process. From results of Fig. 14(b), the performance and stability of MPC is greatly affected by the speed loop response bandwidth. This is because the response delay of the speed loop is uncertain and is not considered in the model of MPC method. To solve this problem, the ideal virtual model is applied in the proposed VM-MPC method. It can be seen from Fig. 14(c) and Fig. 14(e) that the dynamic performance and steady state performance of PD and PF methods are almost unaffected by different speed loop response bandwidths when its values are changed from 100Hz to 40Hz. This is due to their much lower controller gains. However, overshoots of these methods with higher controller gains increase with the decreasing of response bandwidths. This shows that the method to improve the dynamic response of the position loop by increasing controller gains will reduce the robustness. From the experimental results of different methods, it can be seen that a lower controller gain helps to improve the robustness of systems. Using the proposed VM-MPC improves the dynamic response by adding the position advance in the virtual reference without changing controller gains of the position loop, which achieves a balance between the dynamic response and robustness. From the results of robustness test and transient response, both the dynamic response and robustness of the position loop are greatly improved by the proposed VM-MPC strategy.

V. CONCLUSION

In this paper, the virtual reference generated by VM-MPC is proposed to reduce the dynamic tracking error of the position loop without changing position controller gains. The virtual model is used in the proposed MPC method to improve the robustness. A model compensator is used to compensate the mismatch between the virtual model and the real system. Through different reference signal excitation results, it verified that the dynamic tracking error and the settling time are effectively reduced by the proposed algorithm. Moreover, when the speed loop response bandwidth is changed, the control performance of VM-MPC is maintained well. Therefore, the proposed method achieves a balance between dynamic response and robustness, resulting in a better comprehensive performance.

REFERENCES

[1] Z. Ping, T. Wang, Y. Huang, H. Wang, J.-G. Lu, and Y. Li, "Internal model control of PMSM position servo system: Theory and experimental results," *IEEE Trans. Ind. Informat.*, vol. 16, no. 4, pp. 2202–2211, Apr. 2020, doi: 10.1109/TII.2019.2935248.

[2] B. Sarsembayev, K. Suleimenov, and T. D. Do, "High order disturbance observer based PI-PI control system with tracking anti-windup technique for improvement of transient performance of PMSM," *IEEE Access*, vol. 9, pp. 66323–66334, 2021, doi: 10.1109/ACCESS.2021.3074661.

[3] Z. Zhang, L. Jing, X. Wu, W. Xu, J. Liu, G. Lyu, and Z. Fan, "A deadbeat PI controller with modified feedforward for PMSM under low carrier ratio," *IEEE Access*, vol. 9, pp. 63463–63474, 2021, doi: 10.1109/ACCESS.2021.3075486.

[4] J. Z. Shi, "A fractional order general type-2 fuzzy PID controller design algorithm," *IEEE Access*, vol. 8, pp. 52151–52172, 2020, doi: 10.1109/ACCESS.2020.2980686.

[5] F. Khater, A. Shaltout, E. Hendawi, and M. Abu El-sebah, "PI controller based on genetic algorithm for PMSM drive system," in *Proc. IEEE Int. Symp. Ind. Electron.*, Jul. 2009, pp. 250–255, doi: 10.1109/ISIE.2009.5217925.

[6] Z. Yang, J. Du, and S. Zhou, "Position control for filter rod splint based on fuzzy-PID," in *Proc. IEEE Int. Conf. Mechatronics Automat.*, Aug. 2016, pp. 1435–1439, doi: 10.1109/ICMA.2016.7558774.

[7] K. H. Kim, "Model reference adaptive control-based adaptive current control scheme of a PM synchronous motor with an improved servo performance," *IET Electr. Power Appl.*, vol. 3, no. 1, pp. 8–18, Jan. 2009.

[8] C. Wang, X. Shen, J. Xia, and X. Mi, "Model reference adaptive fuzzy neural network control based speed servo system of linear permanent magnet synchronous motor," in *Proc. Int. Conf. Electr. Mach. Syst. (ICEMS)*, Oct. 2007, pp. 1802–1805.

[9] T. Min-an, W. Xiao-Ming, C. Jie, and C. Li, "On Lyapunov stability theory for model reference adaptive control," in *Proc. 4th Int. Conf. Inf. Sci. Control Eng. (ICISCE)*, Jul. 2017, pp. 1055–1060, doi: 10.1109/ICISCE.2017.221.

[10] H. Hongjie and Z. Bo, "A new MRAC method based on neural network for high-precision servo system," in *Proc. IEEE Vehicle Power Propuls. Conf.*, Sep. 2008, pp. 1–5, doi: 10.1109/VPPC.2008.4677480.

[11] G. Cheng and K. Peng, "Robust composite nonlinear feedback control with application to a servo positioning system," *IEEE Trans. Ind. Electron.*, vol. 54, no. 2, pp. 1132–1140, Apr. 2007, doi: 10.1109/TIE.2007.893052.

[12] K. Shyu, C. Lai, Y. Tsai, and D. Yang, "A newly robust controller design for the position control of permanent-magnet synchronous motor," *IEEE Trans. Ind. Electron.*, vol. 49, no. 3, pp. 558–565, Jun. 2002, doi: 10.1109/TIE.2002.1005380.

[13] F. F. M. El-Sousy, "Hybrid H_∞-based wavelet-neural-network tracking control for permanent-magnet synchronous motor servo drives," *IEEE Trans. Ind. Electron.*, vol. 57, no. 9, pp. 3157–3166, Sep. 2010, doi: 10.1109/TIE.2009.2038331.

[14] C.-K. Lai and K.-K. Shyu, "A novel motor drive design for incremental motion system via sliding-mode control method," *IEEE Trans. Ind. Electron.*, vol. 52, no. 2, pp. 499–507, Apr. 2005, doi: 10.1109/TIE.2005.844230.

[15] X. Zhang, L. Sun, K. Zhao, and L. Sun, "Nonlinear speed control for PMSM system using sliding-mode control and disturbance compensation techniques," *IEEE Trans. Power Electron.*, vol. 28, no. 3, pp. 1358–1365, Mar. 2013, doi: 10.1109/TPEL.2012.2206610.

[16] Z. Yin, L. Gong, C. Du, J. Liu, and Y. Zhong, "Integrated position and speed loops under sliding-mode control optimized by differential evolution algorithm for PMSM drives," *IEEE Trans. Power Electron.*, vol. 34, no. 9, pp. 8994–9005, Sep. 2019, doi: 10.1109/TPEL.2018.2889781.

[17] Q. Zou, L. Sun, D. Chen, and K. Wang, "Adaptive sliding mode based position tracking control for PMSM drive system with desired nonlinear friction compensation," *IEEE Access*, vol. 8, pp. 166150–166163, 2020, doi: 10.1109/ACCESS.2020.3022956.

[18] J. Yu, P. Shi, H. Yu, B. Chen, and C. Lin, "Approximation-based discrete-time adaptive position tracking control for interior permanent magnet synchronous motors," *IEEE Trans. Cybern.*, vol. 45, no. 7, pp. 1363–1371, Jul. 2015, doi: 10.1109/TCYB.2014.2351399.

[19] J. Yu, P. Shi, W. Dong, B. Chen, and C. Lin, "Neural network-based adaptive dynamic surface control for permanent magnet synchronous motors," *IEEE Trans. Neural Netw. Learn. Syst.*, vol. 26, no. 3, pp. 640–645, Mar. 2015, doi: 10.1109/TNNLS.2014.2316289.

[20] J. Linares-Flores, C. Garcia-Rodriguez, H. Sira-Ramirez, and O. D. Ramirez-Cardenas, "Robust backstepping tracking controller for low-speed PMSM positioning system: Design, analysis, and implementation," *IEEE Trans. Ind. Informat.*, vol. 11, no. 5, pp. 1130–1141, Oct. 2015, doi: 10.1109/TII.2015.2471814.

[21] G. Prior and M. Krstic, "Quantized-input control Lyapunov approach for permanent magnet synchronous motor drives," *IEEE Trans. Control Syst. Technol.*, vol. 21, no. 5, pp. 1784–1794, Sep. 2013, doi: 10.1109/TCST.2012.2212246.

[22] I. Bélai and M. Huba, "The positional servo drive with the feedforward control and the noise attenuation," in *Proc. Cybern. Informat. (K&I)*, Feb. 2016, pp. 1–6, doi: 10.1109/CYBERI.2016.7438595.

[23] Q. Xu, X. Cheng, H. Yang, Y. Wei, and H. Xue, "Servo control system of permanent magnet synchronous motor based on feedforward control," in *Proc. IEEE 9th Joint Int. Inf. Technol. Artif. Intell. Conf. (ITAIC)*, Dec. 2020, pp. 1799–1804, doi: 10.1109/ITAIC49862.2020.9339046.

[24] S.-H. Choi, J.-S. Ko, I. D. Kim, J.-S. Park, and S.-C. Hong, "Precise position control using a PMSM with a disturbance observer containing a system parameter compensator," *IEE Proc. Electr. Power Appl.*, vol. 152, no. 6, pp. 1573–1577, Nov. 2005.

[25] J. Huang, P. Ma, G. Bao, F. Gao, and X. Shi, "Research on position servo system based on fractional-order extended state observer," *IEEE Access*, vol. 8, pp. 102748–102756, 2020, doi: 10.1109/ACCESS.2020.2997407.

[26] W. Lu, Q. Li, K. Lu, Y. Lu, L. Guo, W. Yan, and F. Xu, "Load adaptive PMSM drive system based on an improved ADRC for manipulator joint," *IEEE Access*, vol. 9, pp. 33369–33384, 2021, doi: 10.1109/ACCESS.2021.3060925.

[27] J. Han, "From PID to active disturbance rejection control," *IEEE Trans. Ind. Electron.*, vol. 56, no. 3, pp. 900–906, Mar. 2009, doi: 10.1109/TIE.2008.2011621.

[28] C.-Y. Lin and Y.-C. Liu, "Precision tracking control and constraint handling of mechatronic servo systems using model predictive control," *IEEE/ASME Trans. Mechatronics*, vol. 17, no. 4, pp. 593–605, Aug. 2012, doi: 10.1109/TMECH.2011.2111376.

[29] S. Chai, L. Wang, and E. Rogers, "A cascade MPC control structure for a PMSM with speed ripple minimization," *IEEE Trans. Ind. Electron.*, vol. 60, no. 8, pp. 2978–2987, Aug. 2013, doi: 10.1109/TIE.2012.2201432.

[30] J. Gao, G. Zhang, P. Wu, X. Zhao, T. Wang, and W. Yan, "Model predictive visual servoing of fully-actuated underwater vehicles with a sliding mode disturbance observer," *IEEE Access*, vol. 7, pp. 25516–25526, 2019, doi: 10.1109/ACCESS.2019.2900998.

[31] Y. Wei, Y. Wei, Y. Sun, H. Qi, and X. Guo, "Prediction horizons optimized nonlinear predictive control for permanent magnet synchronous motor position system," *IEEE Trans. Ind. Electron.*, vol. 67, no. 11, pp. 9153–9163, Nov. 2020, doi: 10.1109/TIE.2019.2955433.

[32] M. Preindl and S. Bolognani, "Model predictive direct speed control with finite control set of PMSM drive systems," *IEEE Trans. Power Electron.*, vol. 28, no. 2, pp. 1007–1015, Feb. 2013, doi: 10.1109/TPEL.2012.2204277.

[33] L. Rovere, A. Formentini, A. Gaeta, P. Zanchetta, and M. Marchesoni, "Sensorless finite-control set model predictive control for IPMSM drives," *IEEE Trans. Ind. Electron.*, vol. 63, no. 9, pp. 5921–5931, Sep. 2016, doi: 10.1109/TIE.2016.2578281.

TAO LIU was born in Hebei, China, in 1994. He received the B.Eng. degree from Xiamen University, Xiamen, China, in 2017, and the M.Eng. degree from the Huazhong University of Science and Technology, Wuhan, China, in 2019, where he is currently pursuing the Ph.D. degree with the School of Optical and Electronic Information.

His current research interests include control of permanent-magnet synchronous machine drives and compensation of voltage-source inverter nonlinearity.

QIAOLING TONG (Member, IEEE) received the B.Eng. and Ph.D. degrees from the School of Optical and Electronic Information, Huazhong University of Science and Technology, China, in 2003 and 2010, respectively. From 2008 to 2010, he was a Research Scholar with the Department of Electrical Engineering and Computer Science, University of California, Irvine. He is currently an Associate Professor at the School of Optical and Electronic Information, Huazhong University of Science and Technology. His current research interests include sensorless control of DC–DC converters and VLSI implementation of intelligent algorithms.

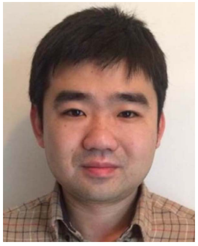

QIAO ZHANG (Member, IEEE) received the B.Eng., M.Eng., and Ph.D. degrees from the Huazhong University of Science and Technology, Wuhan, China, in 2003, 2006, and 2010, respectively. From 2008 to 2009, he was a Visiting Scholar with the Department of Electronic and Electrical Engineering, The University of Sheffield, U.K. From 2009 to 2016, he was a Research Engineer at the IMRA Europe U.K. Research Centre. He is currently an Associate Professor at the School of Automation, Wuhan University of Technology. His research interests include the power electronics system design and control, such as dc–dc converter sensorless control strategies, electrical machine parameters estimation by control theory, system nonlinearity compensation for dc–dc converters, and voltage source inverters.

KAN LIU (Senior Member, IEEE) received the B.Eng. and Ph.D. degrees in automation from Hunan University, Changsha, China, in 2005 and 2011, respectively, and the Ph.D. degree in electronic and electrical engineering from The University of Sheffield, Sheffield, U.K., in 2013.

From 2013 to 2016, he was a Research Associate with the Department of Electronic and Electrical Engineering, The University of Sheffield. From 2016 to 2017, he was a Lecturer with the Control Systems Group, Loughborough University. He is currently a Professor of electro-mechanical engineering with Hunan University. His research interests include parameters estimation and sensorless control of permanent magnet synchronous machine drives, advanced design, and control solutions of high-power density converters, for applications ranging from electric locomotive and automotive to servo motor and drive.

Prof. Liu is the Director of the Engineering Research Center of Ministry of Education on Automotive Electronics and Control Technology, China. He serves as an Associate Editor for IEEE ACCESS and the *CES Transactions on Electrical Machines and Systems*.